Available online at www.sciencedirect.com
SCIENCE DIRECT
Polymer Degradation and Stability 91 (2006) 1861–1869
Polymer Degradation and Stability
www.elsevier.com/locate/polydegstab

Modeling of oxidative development in PMR-15 resin

G.P. Tandon [a,*], K.V. Pochiraju [b], G.A. Schoeppner [c]

[a] University of Dayton Research Institute, Nonmetallic Materials Division, 300 College Park, Dayton, OH 45469-0168, United States
[b] Stevens Institute of Technology, Hoboken, NJ 07030, United States
[c] AFRL/MLBC, WPAFB, OH 45433-7750, United States

Received 10 May 2005; received in revised form 9 November 2005; accepted 9 November 2005
Available online 23 January 2006

Abstract

A multidisciplinary approach focused on models and processes to predict the performance and life expectancy of high-temperature polymer matrix composite (HTPMC) materials used in a variety of aerospace applications is being developed. Emphasis is on the implementation and extension of hierarchical models to represent the polymer behavior/properties as a function of the degradation state. Neat resin specimens of high-temperature polyimide PMR-15 have been evaluated for various aging conditions. Characterization of the properties of the polyimide is focused on development of a constitutive law for use in a micromechanical analysis to predict the behavior of PMR-15 reinforced composites. Thermo-oxidative aging is simulated with a diffusion-reaction model in which temperature, oxygen concentration and weight loss effects are considered. One-dimensional simulations illustrate oxidative layer growth for neat resin specimens. Comparisons and correlations with experimental observations of oxidation layer growth are presented.

Keywords: Aging; Degradation; Durability; Thermal oxidation

1. Introduction

Polymer matrix composites (PMCs) operating in high-temperature environments (100–350 °C) undergo thermo-oxidative degradation and accelerated damage evolution. Several researchers in the composites community e.g., [14,18] are working on the model-based design and development of novel material systems that enhance the life and affordability of HTPMCs. Mechanism-based models e.g., [4,10,21,22] are expected to yield an understanding of the mechanisms behind observed degradation phenomenon, help to design accelerated tests and are a first step towards a predictive capability. The high-temperature aging behavior of several neat polymer resins has been studied [1–3,20]. Several major aging mechanisms can be identified that lead to weight loss and damage growth and hence degradation of the performance of the resin. They are:

- *Physical aging*: The thermodynamically reversible volumetric response due to slow evolution toward thermodynamic equilibrium is identified as physical aging. The decreased molecular mobility and free-volume reduction lead to strain and damage development in the structure.
- *Chemical aging*: The nonreversible volumetric response due to chain-scission reactions and/or additional crosslinking (not associated with reactions with oxygen), hydrolysis, depolymerization and plasticization is classified as chemical aging.
- *Thermo-oxidative aging*: The nonreversible surface diffusion response and chemical changes occurring during oxidation of a polymer (hence a modality of chemical aging) are termed as oxidative or thermo-oxidative aging of the polymeric matrix. The oxidative aging may lead to either the reduction in molecular weight as a result of

* Corresponding author. Tel.: +1 937 255 1393; fax: +1 937 258 8075.
E-mail address: g.tandon@wpafb.af.mil (G.P. Tandon).

0141-3910/$ - see front matter © 2005 Elsevier Ltd. All rights reserved.
doi:10.1016/j.polymdegradstab.2005.11.008

chemical bond breakage and loss in weight from outgassing of low molecular weight gaseous species or chain scissation and formation of dangling chains in networks.

- *Mechanical stress-induced aging*: Mechanical and thermal fatigue loading cause micromechanical damage growth within the material. The damage evolution in turn acerbates the creep and thermo-oxidative response of the material. This aging mechanism is the least understood and least modeled by researchers.

Recent studies e.g., [3,16,19] document the growth of the thermo-oxidative layer and the changes in elastic moduli and chemical composition resulting from isothermal aging in oxidizing environments in high-temperature polyimide resins. It has been observed that the polymer degradation occurred mainly within a thin surface layer that developed and grew during thermal aging. In general, the core of thick (2+ mm) polymer specimens was protected from oxidative degradation during the tested length of exposure and was relatively unchanged by the thermal treatment. An associated problem is the crack initiation and damage growth in the oxidized matrix region. Embrittlement of the surface layer induced by thermal oxidation leads to a density increase and a weight loss; both processes contribute to the shrinkage of the oxidized layer which generates tensile stresses and possibly "spontaneous" cracks [2,5,11,13]. The crack faces provide additional diffusion surfaces and accelerate the material degradation and growth of the oxidation layer [16].

To accurately predict the performance of PMC components, knowledge of the individual aging mechanisms, their synergistic effects and the spatial variability of the thermo-oxidative degradation are critical. In this work, thermo-oxidative aging is simulated with a diffusion/reaction model in which temperature, oxygen concentration and weight loss effects are considered. A parametric reaction model based on a mechanistic view of the reaction is used for simulating reaction rate dependence on the oxygen availability in the polymer. This paper gives an extension of the kinetic model proposed by Colin et al. [6,7], describing the thermal oxidation kinetics of polymers in the stationary state (i.e., in the domain of the low conversion ratios). The extension concerns the domain of high conversion ratios in which the constancy of the substrate concentration is no longer valid. Indeed, the substrate depletion leads to an auto-retardation of the oxidation kinetics. A practical consequence is a decrease of the oxidation rate in the superficial layers of the specimen, where the high conversion ratios are firstly reached, which leads to a moving of the oxidation front towards the specimen core. Such an extension was proposed by Colin et al. [8,9] and successfully applied to the thermal oxidation of amine crosslinked epoxy and bismaleimide. The system of differential equations constituting the kinetic model, in which was added a new equation describing the substrate depletion, was solved numerically without any simplifying assumptions (concerning the long kinetic chains, the stationary state or the existence of a relationship between the termination rate constants). This new model accurately predicted the continual increase of the thickness of oxidized layer in the domain of high conversion ratios.

In this paper, we have proposed another extension. We assume that the expression of the oxygen consumption rate determined in the stationary state remains valid in the domain of high conversion ratios. The oxygen consumption expression contains two key parameters of the oxidation kinetics: (i) the maximal oxidation rate in oxygen excess $R_0 = (k_3^2[\mathrm{PH}]^2)/k_6$; and (ii) the reciprocal of the critical oxygen concentration beyond which oxygen excess is reached: $\beta = k_2k_6/(2k_5k_3[\mathrm{PH}])$. It is clear that both parameters are linked to the substrate concentration [PH]. However, we assume that only R_0 is especially affected by the substrate depletion. For this paper, macroscopic weight loss measurements are used to determine the reaction and polymer consumption parameters. We compare and correlate the experimental oxidation layer growth in high-temperature polyimide resin with parametric analyses obtained from simulations. Results from this work will be subsequently utilized to link the diffusion-reaction models of chemical and thermo-oxidative degradation with micromechanical analysis and for development of a constitutive law to predict the behavior of HTPMC.

2. Modeling of thermo-oxidation

Fig. 1 shows the various mechanisms of the thermo-oxidative degradation of the composite. Note that the illustrations show the mechanisms as individual events. However, in reality, the mechanisms are coupled, some may dominate more compared to others, and the sequence of their occurrence could be a function of the material property and the aging environment (i.e., temperature, pressure, etc.). When the material is first exposed to the oxidizing environment, the boundary sorption (controlled by Henry's law) will determine the solubility of the gas into the material. We will assume, as a first approximation, that the transport of the gas within the material is controlled by Fickian diffusion. The adsorbed oxygen diffuses into the volume and is followed by reaction of the polymer. The rate of reaction is modeled as a function of both the oxygen availability (through

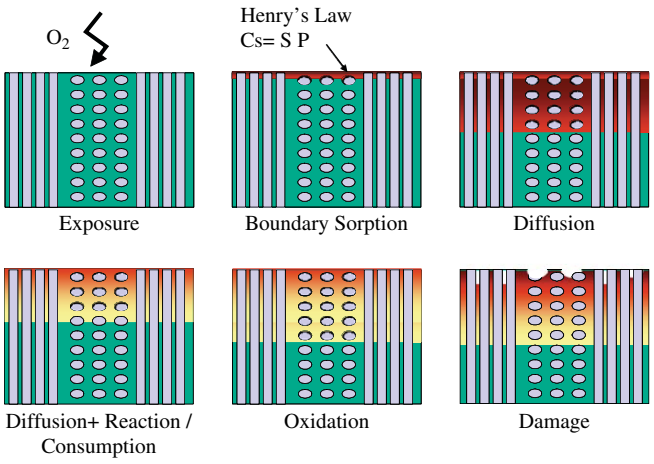

Fig. 1. Six phases of thermo-oxidative damage evolution which include exposure to oxygen environment, sorption at the boundary, diffusion/reaction, oxidative layer growth and material damage.

diffusion) and the polymer availability (tracking end products of reaction), besides being dependent on temperature.

2.1. Sorption and diffusion modeling

With $C(x,y,z;t)$ denoting the concentration field at any time within a domain with a diffusivity of D_{ij} and consumptive reaction with a rate $R(C)$, the diffusion reaction with orthotropic diffusivity is given by Eq. (1)

$$\frac{\partial C}{\partial t} = \left(D_{11}\frac{\partial^2 C}{\partial x^2} + D_{22}\frac{\partial^2 C}{\partial y^2} + D_{33}\frac{\partial^2 C}{\partial z^2} \right) - R(C) \tag{1}$$

subjected to the boundary conditions

$C = C^{\mathrm{s}}$ on the exposed boundaries

$$\frac{\mathrm{d}C}{\mathrm{d}t} = 0 \text{ on symmetry boundaries}$$

The boundary sorption on the exposed boundaries is given by Henry's equation

$$C^S = SP \tag{2}$$

where S is the solubility and P is the partial pressure of the oxygen in the environment. The diffusivities are temperature dependent typically given in Arrhenius form:

$$D_{ij} = D_{ij}^0 \exp(-E_{\mathrm{a}}/\mathrm{R}T) \tag{3}$$

and are determined using permeability tests at lower temperatures to determine the pre-exponent (D_{ij}^0) and the activation energy parameters (E_{a}). Assuming isotropic diffusion, Table 1 shows the values of these parameters for a typical high-temperature polyimide resin as determined by Abdeljaoued [1] in its virgin state, i.e., unoxidized condition, where the subscript on the pre-exponent have been omitted for brevity.

2.1.1. Heterogeneity in diffusivity

Thermo-oxidative aging of the polymeric material will change the chemical composition of the polymer and hence the physical properties of the material. Therefore, any part of the polymer subjected to thermo-oxidation will invariably contain multiple material phases – namely, the unoxidized or virgin polymer, the active reaction zone (where a mix of oxidized and unoxidized polymers exist) and an oxidized polymer phase. Although this three-phase model is analogous to the two-phase models (or skin/core models) described earlier [15,17], the description of three phases enables extension to situations with high conversion ratios in which the constancy of the substrate concentration is no longer valid. Indeed, the substrate depletion leads to an auto-retardation of the oxidation kinetics. A practical consequence is a decrease of the oxidation rate in the superficial layers of the specimen, where the high conversion ratios are firstly reached, which leads to the growth of the oxidation front towards the specimen core. In general, the diffusivities for each of these phases will be different, while the diffusivity of the oxidized polymer layer is the controlling parameter as the diffusion of oxygen through the oxidized layer is the source of oxygen supply to the unoxidized layer. In this work several simulations of oxidation layer growth will be presented. Initially, for lack of better information, we will assume that the diffusivities for the three phases are the same and equal to the unoxidized value. Later, we will consider the case where the diffusivity D_{ij} at a material location is assumed to be a linear interpolation of the diffusivities of the oxidized and unoxidized materials, denoted by D_{ij}^{ox} and D_{ij}^{un}, respectively. For the remainder of this paper, superscripts ox and un will be used with diffusivity values whenever needed for clarity.

Table 1
Constants for evaluating diffusivity of polyimide resin

	Unoxidized, $\phi = 1$([1])
D_0	6.10×10^{-11} m^2/s
E_{a}	19 700 J/mol
R	8.31447 J/(mol K)

2.2. Reaction modeling

The reaction rate term, $R(C)$, in Eq. (1), models the reaction of the oxygen with the polymer. Oxygen can react with the end caps of the polymer and/or the backbone of the polymer. The reaction modeling presented here assumes that the reaction products (water and other volatiles) leave the polymer instantaneously and no modeling of the outgassing is conducted. The reaction rate depends upon temperature and oxygen concentration. While the Arrhenius-type kinetics models e.g., [14] are suitable for capturing the temperature, the mechanistic models [1,6,7] capture the reaction rate dependence on the concentration dependence as well. The mechanistic models typically determine the reaction rate based on a saturation reaction rate (R_0) when the reaction is not oxygen deprived. The reaction rate is reduced when the oxygen availability is reduced, namely,

$$R(C) = R_0 f(C) \tag{4}$$

where R_0 is the saturation reaction rate. The function $f(C)$ in Eq. (4) models the situation in which the amount of oxygen available for reaction is lower than that required for the maximum reaction rate reached under saturation conditions. The reduction in reaction rate can be modeled following Colin et al. [6,7] using Eq. (5).

$$f(C) = \frac{2\beta C}{1+\beta C}\left[1 - \frac{\beta C}{2(1+\beta C)}\right] \tag{5}$$

Fig. 2 shows the dependence of the reaction rate on the concentration as modeled by Eq. (5). The abscissa has a normalized concentration parameter (βC) in which the parameter, β, nondimensionalizes the concentration field. According to Eq. (5), there is a rapid acceleration phase $(0 < \beta C < \sim 3)$ and a relative constant phase $(\beta C > 3)$. For this analysis, we chose this simpler, two-phase, reaction rate to concentration dependence.

The oxygen consumption expression contains two key parameters of the oxidation kinetics: (i) the maximal oxidation

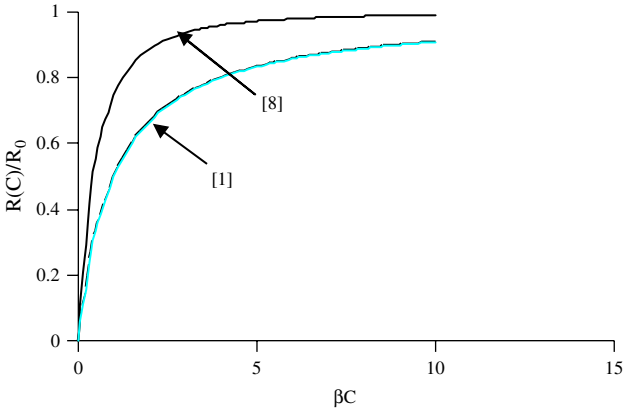

Fig. 2. Typical model of reaction rate dependence on concentration.

rate in oxygen excess $R_0 = k_3^2[\mathrm{PH}]^2/k_6$; and (ii) the reciprocal of the critical oxygen concentration beyond which oxygen excess is reached: $\beta = k_2k_6/2k_5k_3[\mathrm{PH}]$. It is clear that both parameters are linked to the substrate concentration [PH]. However, we assume that only R_0 is especially affected by the substrate depletion, which could be justified by the fact that [PH] appears with an exponent 2 in R_0, whereas it appears only with an exponent 1 in β.

The value of β can be determined from weight loss data obtained at two oxygen partial pressures, typically in pure O_2 and in air. In order to determine this value, we need weight loss measurements at two concentrations which translate to the reaction rates at those two concentration values. Since the weight loss is taken to be proportional to the oxygen consumption rate, the ratio of the weight loss determined at two concentrations is the same as $R_1(C_1)/R_2(C_2)$. For example, from Abdeljaoued [1], the ratio of the weight loss between pure O_2 ($C_1 = 3.74$ mol/m^3) and air ($C_2 = 0.79$ mol/m^3) is about 0.7 at 280 °C over 40–170 h of aging. Therefore,

$$\frac{2\beta C_1}{1+\beta C_1}\left[1-\frac{\beta C_1}{2(1+\beta C_1)}\right] = 0.7\frac{2\beta C_2}{1+\beta C_2}\left[1-\frac{\beta C_2}{2(1+\beta C_2)}\right] \tag{6}$$

Solving the equations produces three roots: [*−3.5593*, *−0.42657*, *0.91947*], with only one physically feasible value for the polyimide resin, $\beta \approx 0.919$.

2.3. Oxidation layer growth modeling

The simulation of the oxidation layer growth requires the specification of the reaction rate R_0 and a mechanism for reaction completion/cessation. Considering that the oxidation reaction will stop if it is oxygen-starved as modeled by Eq. (5), the reaction will stop when all the active polymer sites are consumed. In the latter case, the oxygen will again diffuse deeper into the material in favor of the reaction. In this section we describe the case when the diffusing oxygen finds the active polymer reaction sites creating an active oxidation layer followed by advancement of the layer upon the reaction completion.

2.3.1. Active oxidation layer size

Under the assumption that abundant active sites are available for reaction in the polymer, the diffusion-reaction equation (Eq. (1)) leads to a zone over which oxidation takes place. This zone will be proportional to the ratio of the volume in which oxygen has diffused over the volume where it has reacted. For the polyimide resin under consideration, the active reaction zone forms quickly (can be seen within 1 h). The optical experimental observations reported by Ripberger et al. [16] also verify the existence of a zone between the oxidized and unoxidized regions.

Fig. 3 shows the active reaction zone measurements for polyimide resin at 288 °C. This figure shows two distinguishable region sizes – namely 17 μm before 40 h and 25 μm after 40 h of aging. These active reaction zone sizes correspond to a R_0 value of about 3.5 mol/m^3 min for the first 40 h of aging which then slows down to a reaction rate corresponding to about 2 mol/m^3 min. We recognize that the reaction zone size will grow from an initial value of zero at the start of aging to a finite value (which can be experimentally observed and measured) over a period of time. However, for simplicity, the measured active reaction zone size has been fitted to correspond to two constant R_0 values.

2.3.2. Reaction termination criterion

While the active zone modeling describes the reaction rate and its dependence on oxygen availability (concentration fields), the diffusion-reaction system will be stationary (does not grow into the polymer thickness) if sufficient amount of polymer is available for reaction. However, under longer-term (tens to hundreds of hours) aging conditions, the oxidation layer will grow moving the active reaction zone into the polymer, and three zones can be observed along the depth of the polymer, as illustrated in Fig. 4. Therefore, a polymer availability state variable (ϕ) is defined which indicates the availability of an active polymer site for reaction. The state variable ϕ is parameterized to vary from $\phi_{ox} < \phi < 1$, where ϕ_{ox} denotes completely oxidized polymer, and $\phi = 1$ denotes unoxidized polymer. We assume that the reaction is terminated when ϕ equals ϕ_{ox}.

In this effort, we utilize the weight loss information to determine the value of ϕ_{ox}. In order to determine this value,

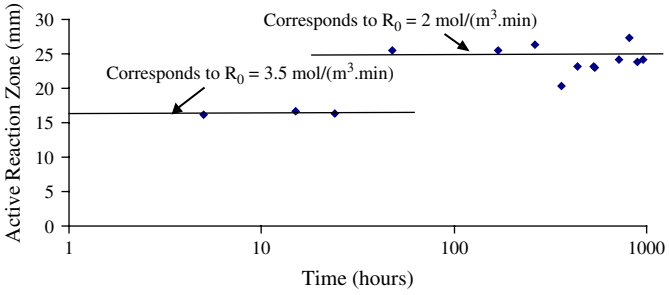

Fig. 3. Active reaction zone variation with time illustrating slowing of the oxidation reaction after 40 h of aging.

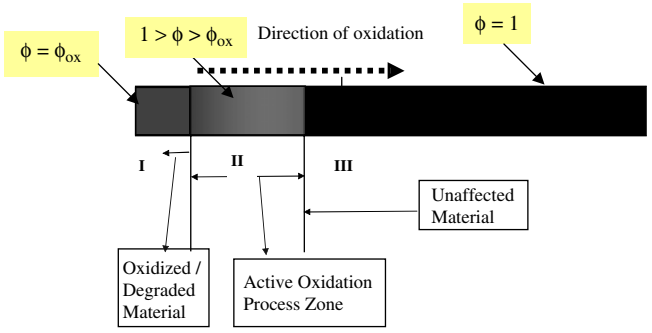

Fig. 4. Schematic of the three zones in thermo-oxidation. The oxidized region is followed by active zone separating the oxidized and unoxidized regions.

first we must establish a relation between the oxidation layer size and the weight loss. The most common assumption relating the two parameters is that the weight loss rate (dW/dt) is proportional to the reaction rate $R(C)$, i.e.,

$$\frac{dW}{dt} \propto -R(C) \tag{7}$$

where the negative sign is introduced in Eq. (7) since the weight loss is negative and the oxygen consumption rate is positive. We now define an oxidation state parameter at any point in the material as the current weight of the material over its original (unoxidized) weight, i.e., $\phi = (W(t))/W_0$. Thus,

$$\frac{d\phi}{dt} = \frac{1}{W_0}\frac{dW}{dt} \tag{8}$$

Combining Eqs. (7) and (8), we obtain,

$$\frac{d\phi(t)}{dt} = -\alpha R(C) \tag{9}$$

where a constant of proportionality (α) relates the oxidation state change ($d\phi/dt$) and the reaction rate ($R(C)$). The parameters, ϕ_{ox} and α, can be determined from the weight loss data for known specimen geometry together with oxidation layer size data measurements.

2.4. Determination of ϕ_{ox} from weight loss experimentation

In an inert environment, post-polymerization and thermolysis are the two typically active mechanisms, whereas in an oxidizing environment thermo-oxidation is also present. Therefore, aging experiments are conducted both in inert atmospheres (e.g., argon) and oxidative atmospheres (air), and the weight loss is recorded at various time intervals in order to determine the effect of oxidation on aging. Let the initial specimen dimensions be given by length (L), width (W) and thickness (T). At a particular time interval if the weight loss fraction (weight loss/original weight) in the inert atmosphere is given as γ, and weight loss fraction after the same time period in air is given by ε, then the weight loss fraction due to oxidation alone is ($\varepsilon-\gamma$). Let the observed thickness of the completely oxidized layer and the active oxidation layer be denoted by t_o, and t_a, respectively, as shown in Fig. 5. The initial volume of the specimen (V), the volume of the fully oxidized zone (V_o), and the volume of the active oxidation zone (V_a) are therefore, given by:

$$\begin{aligned} V &= LWT \\ V_o &= \{LWT - (L-2t_o)(W-2t_o)(T-2t_o)\} \\ V_a &= \{LWT - V_o - (L-2(t_a+t_o))(W-2(t_a+t_o))(T-2(t_a+t_o))\} \end{aligned} \tag{10}$$

Assuming that the oxidative weight loss is confined to the oxidation zone and that ϕ_{ox} varies linearly in the active oxidation zone, the weight loss in the oxidized zone should therefore, be equal to the weight loss in the specimen, i.e.,

$$\left[(1-\phi_{ox})V_o + \left(\frac{1-\phi_{ox}}{2}\right)V_a\right]\rho = (LWT)[\varepsilon-\gamma]\rho \tag{11}$$

where ρ is the density. Solving for ϕ_{ox}, we obtain

$$\phi_{ox} = 1 - \frac{V(\varepsilon-\gamma)}{V_o + \frac{1}{2}V_a} \tag{12}$$

Eqs. (10)–(12) determine the value of ϕ_{ox} from oxidation layer size observations and weight loss data determined from aging in inert (γ) and oxidative (ε) environments.

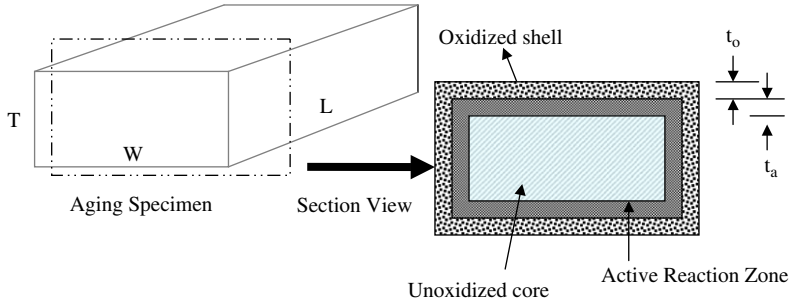

Fig. 5. Geometry of the specimen used for aging with all boundaries exposed to oxygen. The oxidized layer, active reaction zone and the unoxidized regions are illustrated in the sectional view.

3. Numerical thermo-oxidation simulation

The diffusion-reaction system of equations is solved using numerical solutions to differential algebraic equations in a 1-D domain. These methods are computationally effective when performing parametric sensitivity analysis. This section describes the solution algorithms used to solve the diffusion-reaction system with the reaction rate following Eq. (5) described as follows:

$$R(C) = \begin{cases} R_0 2\xi\left(1-\dfrac{\xi}{2}\right) & \text{for} \quad \phi < \phi_{ox} \\ 0 & \text{for} \quad \phi = \phi_{ox} \end{cases} \qquad (13)$$

$$\text{where} \quad \xi = \frac{\beta C}{1+\beta C}$$

The diffusion-reaction system is solved using modified implementation of *ode15s* and *pdepe* solvers in the MATLAB™ system. The oxidation-dependent diffusivity $D_{ij}(\phi)$ is determined at each computational point using the model discussed in Section 2.1.1, namely,

$$D_{ij}(\phi) = D_{ij}^{un}\frac{(\phi-\phi_{ox})}{(1-\phi_{ox})} + D_{ij}^{ox}\frac{(1-\phi)}{(1-\phi_{ox})} \qquad (14)$$

The oxidation state variable (ϕ) is determined at every time step during the computation using the weight loss relationship shown in Eq. (15),

$$\phi = \min\left\{\phi_{ox}, \left(1 - \int_0^t \alpha(\zeta)R(\zeta)\mathrm{d}\zeta\right)\right\} \qquad (15)$$

The system of diffusion-reaction formulation given in Eq. (1) is solved using numerical methods. The mesh used has 1.6 μm spacing in the spatial domain and automated time stepping with a minimum time step of 1×10^{-6} min and a maximum time step of 2.5×10^{-3} min. A typical solution takes on the order of 20 min of CPU time on a desktop computer with 2.8 GHz Intel™ CPU and 512 MB RAM.

4. Thermo-oxidative behavior of PMR-15 resin

In order to understand the thermo-oxidative behavior of the polymer, we compare and correlate the experimental oxidation layer growth obtained at 288 °C (550 °F) with parametric analyses obtained from simulations. These comparisons provide quantitative values for various parameters of the model, especially the temperature-dependent saturation reaction rate (R_0), the behavior of the proportionality (α) between reaction rate and the weight loss, the polymer availability state variable ϕ_{ox}, and the apparent diffusivity of the oxidized region (D_{ij}^{ox}).

A diffusivity value of 53.6×10^{-6} mm^2/min is calculated for PMR-15 resin at 288 °C (550 °F) using Eq. (3) in conjunction with the unoxidized pre-exponent (D_0) and the activation energy parameters (E_a) listed in Table 1. The value of ϕ_{ox} as determined from the experimental weight loss data was not found to be constant but observed to decrease with aging time. Material loss from the edges and volumetric shrinkage is both observed during oxidative aging experiments, and these effects are predominant beyond 100 h of aging. Therefore, the ϕ_{ox} value is determined by averaging the predictions during the initial time period of 100 h at 288 °C. The average ϕ_{ox} value as determined by Eq. (12) and experimental weight loss data is 0.187, which means that the completely oxidized polymer weighs about 18.7% of the unoxidized polymer.

4.1. Influence of saturation reaction rate, R_o

Fig. 6 shows the experimental observations and the predictions of oxidation layer growth at 288 °C (550 °F). The simulations shown are with a constant diffusivity ($D_{ij}^{un} = D_{ij}^{ox} = 53.6 \times 10^{-6}$ mm^2/min) and a constant value of the proportionality constant ($\alpha = 0.3$). Several values of reaction rates (5.5 mol/m^3 min, 3.5 mol/m^3 min, 0.5 mol/m^3 min) are considered. The oxidation layer growth predictions show little dependence on the reaction rate R_0. Moreover, the simulations overpredict the oxidation layer growth at longer aging times. As mentioned earlier, the choice of saturation reaction rate mainly influences the size of the active reaction zone. A larger reaction rate results in a decrease in the size of the active zone, whereas a smaller value results in an increase in the size of the active reaction zone. The experimental measurements of [16] support larger reaction rates during the initial aging period which then decrease at longer aging times.

4.2. Influence of polymer availability state variable, ϕ_{ox}

Fig. 7 shows the influence of ϕ_{ox} on oxidation layer growth predictions using constant values of $D_{ij}^{un} = D_{ij}^{ox} = 53.6 \times 10^{-6}$ mm^2/min, $R_0 = 3.5$ mol/m^3 min and $\alpha = 0.3$. An average ϕ_{ox} value of 0.187 was determined using the weight loss data during the initial 100 h of aging. For this figure, two other constant ϕ_{ox} values, namely, 0.1 and 0.3, were considered. Clearly, the oxidation layer predictions are seen to increase with

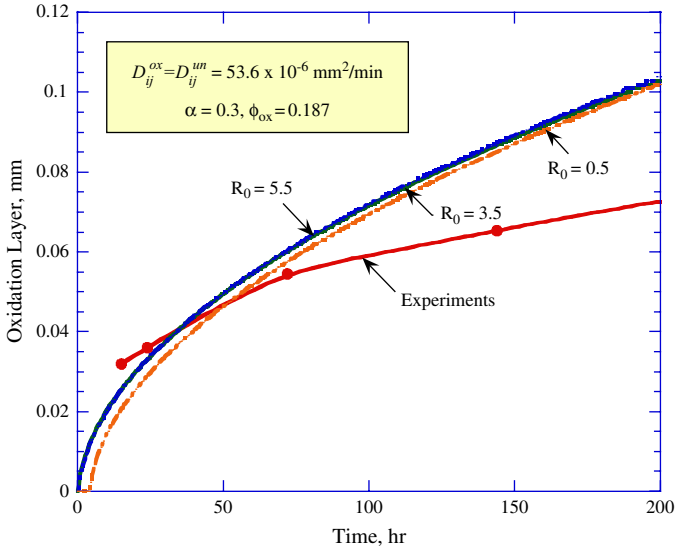

Fig. 6. Influence of R_0 on oxidation layer growth predictions.

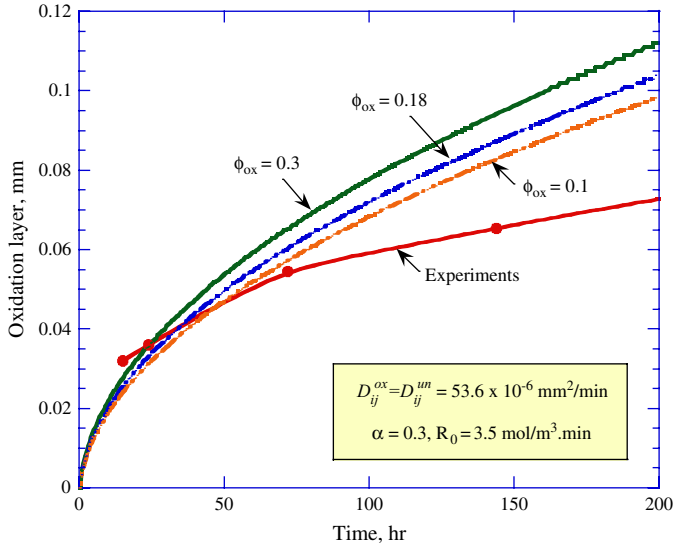

Fig. 7. Influence of ϕ_{ox} on oxidation layer growth predictions.

increase in the value of ϕ_{ox}. A larger value of ϕ_{ox} implies earlier cut-off of polymer availability for reaction leading to an advancement of the reaction zone and larger oxidation layer thickness.

4.3. Influence of proportionality factor, α

Fig. 8 shows the influence of α on oxidation layer growth predictions using a constant diffusivity ($D_{ij}^{un} = D_{ij}^{ox} = 53.6 \times 10^{-6}$ mm^2/min) and a constant value of the saturation reaction rate ($R_0 = 3.5$ mol/m^3 min). Initially, we assume that the proportionality factor α is constant with time (i.e., aging). As seen in Fig. 8, a larger value of α predicts the data well at small aging times but clearly overpredicts at longer aging times. On the other hand, a smaller value of α vastly underpredicts at smaller aging times but gives a better fit at longer aging time periods. This therefore, leads us to believe that the weight loss proportionality factor (α) is not a constant but depends upon the oxidative aging time. In the third simulation shown in Fig. 8, we therefore, assume α to vary linearly from a value of 0.3 to 0.1 within the first 40 h and keep it constant beyond that time. With this assumed variation (which is in agreement with larger weight loss rates observed during the beginning of the experiments), the numerical simulations of oxidation layer growth are still underpredicted, but the shape of the predicted curve is now offset from the measurements by a small amount. The proportionality between the oxygen consumption rate and weight loss rate was established by Abdeljaoued [1] using simplifying assumptions of which some of them (e.g., existence of a relationship between termination rate constants) were rejected by Gillen et al. [12]. Thus, a value of α which does not remain constant with time, as seen from our simulations, bodes well with the findings of Gillen et al. [12].

4.4. Influence of diffusivity, D_{ij}^{ox} and D_{ij}^{un}

Fig. 9 shows the experimental oxidation layer growth data at 288 °C compared with several simulations with varying diffusivity. We initially assume that the diffusivity of the oxidized material is the same as the diffusivity of the material in its virgin state, i.e., unoxidized condition. On increasing the constant diffusivity value from 53.6×10^{-6} mm^2/min to 78×10^{-6} mm^2/min (i.e., setting $D_{ij}^{un} = D_{ij}^{ox} = 78 \times 10^{-6}$ mm^2/min), the predictions overestimate the oxidation layer even further at longer aging times. The behavior worsens even further using $D_{ij}^{un} = D_{ij}^{ox} = 100 \times 10^{-6}$ mm^2/min. Next, we increase the diffusivity value in the oxidized region from 53.6×10^{-6} mm^2/min to 78×10^{-6} mm^2/min and keep $D_{ij}^{un} = 53.6\times 10^{-6}$ mm^2/min. This simulation differs very little from our earlier simulation with $D_{ij}^{un} = D_{ij}^{ox} = 78 \times 10^{-6}$ mm^2/min, and therefore, illustrates that the oxidation region growth is predominantly controlled by the diffusivity of the oxidized region and is far less sensitive to the diffusivity of the unoxidized material. In the case of low conversion ratios, it is generally assumed that the

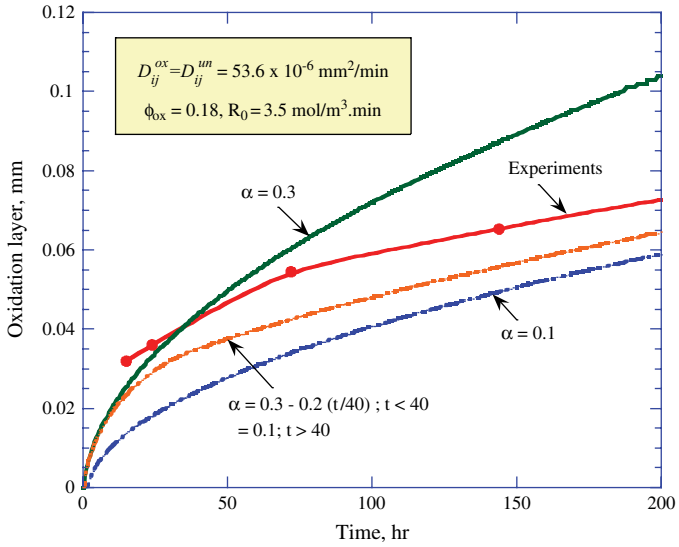

Fig. 8. Influence of α on oxidation layer growth predictions.

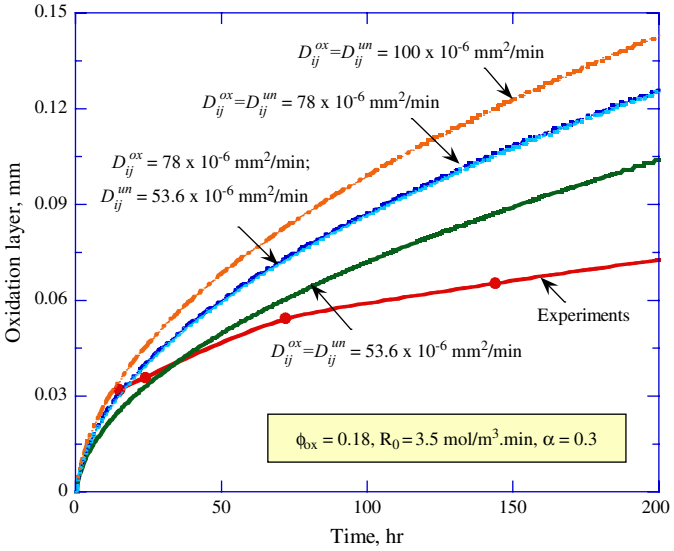

Fig. 9. Influence of diffusivity on oxidation layer growth predictions.

oxygen diffusivity does not change. This assumption has been checked experimentally for some linear polymers (PP and PE) and thermosets (epoxy). However, the problem remains totally open in the case of high conversion ratios. But, it can be reasonably considered, in a first approximation, that the diffusivity increases when the chemical structure changes a lot (presence of many oxygenated species) and the network is almost destroyed (presence of many dangling chains). As a result, it can be reasonably imagined that oxygen diffusivity increases notably in the superficial layers where high conversion ratios are reached.

4.5. Combined influence of controlling parameters

If the diffusivity of the resin is left unchanged with $D_{ij}^{un} = D_{ij}^{ox} = 53.6 \times 10^{-6}$ mm^2/min, but α is assumed to vary linearly from a value of 0.3 to 0.1 within the first 40 h and kept constant beyond that time, the numerical simulations of oxidation layer growth are underpredicted, but the shape of the predicted curve is approximately parallel to the experimental measurements. Next, if we increase the diffusivity value in the oxidized region from 53.6×10^{-6} mm^2/min to 78×10^{-6} mm^2/min and keep $D_{ij}^{un} = 53.6 \times 10^{-6}$ mm^2/min in conjunction with a linear variation of α for the first 40 h, we now obtain a very good agreement between the predictions and the measurements of the oxidation layer, as seen in Fig. 10. This good matching therefore, gives credence to our assumptions that the diffusivity values within the oxidized region are larger compared to the values in the unoxidized region, and that the value of α changes with aging with a larger value obtained initially, which is also in agreement with larger weight loss rates observed during the beginning of the experiments.

4.6. Extrapolations to longer aging times

In order to project the oxidation layer growth to thousands of hours of aging, we use extrapolations from the simulation of first

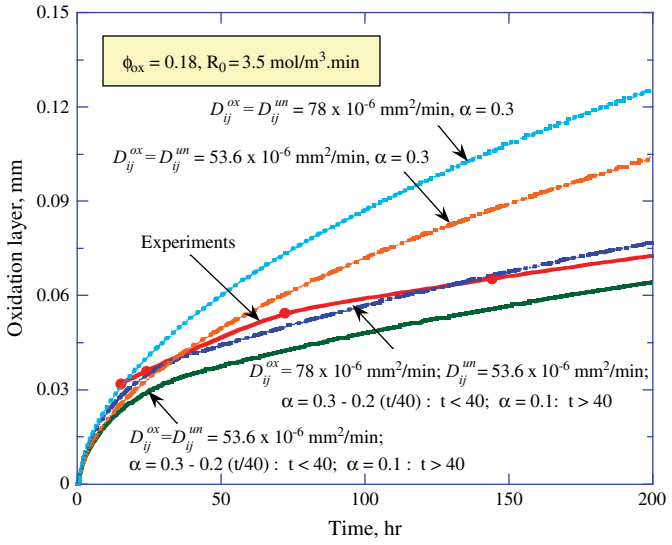

Fig. 10. Combined influence of controlling parameters on oxidation layer growth predictions.

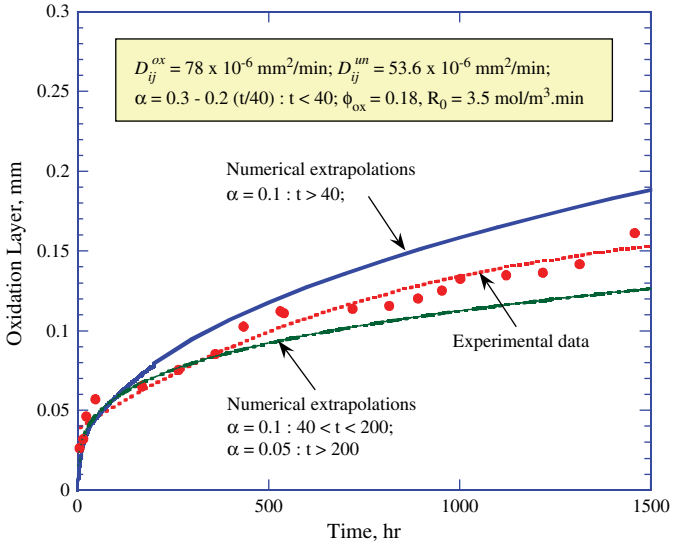

Fig. 11. Comparison of extrapolated oxidation layer growth predictions with measurements.

200 h of the oxidation layer growth. The oxidation layer size is fitted using a power law dependence with time and the long term predictions are obtained by extrapolation. The oxidation layer size, extrapolated to 1500 h of aging, is compared with experimental measurements in Fig. 11. The values of the parameters used in the simulations are also listed in the figure. The results indicate that the comparisons, using a constant $\alpha = 0.1$ beyond 40 h of aging, are reasonable for 500 h of aging but are overestimated at longer time periods. However, when we simulated the layer growth by reducing the value of α from 0.1 to 0.05 for aging from 200 h to 400 h, the predictions are underestimating the oxidized layer thickness at longer aging times. These extrapolations and comparisons for longer aging times therefore, illustrate that the proportionality factor (α) is not a constant but depends upon the aging time. Further work is needed to help establish this correspondence from the weight loss data.

5. Concluding remarks

A comprehensive and predictive model for thermo-oxidation of high-temperature polymers has been formulated. The model considers diffusion, reaction and oxidation of the resin system. This work extends the earlier mechanistic models by introducing the concept of polymer availability, thereby producing predictive oxidation layer growth simulations. The parameters utilized in the model and their relations to physically observable behavior are described.

Parametric studies are conducted to examine the sensitivity of the controlling parameters. It is observed that the oxidation growth process is clearly diffusion controlled, and the diffusivity of the oxidized region is the controlling parameter. The parameter, α, relates the reaction rate to the weight loss rate of the polymer, and the parameter ϕ_{ox} is the normalized weight of the completely oxidized polymer at which the oxidation reaction terminates. This weight loss rate to reaction rate relationship

is essential to measure the progress of the oxidation reaction rate through bulk specimen aging and oxidation experiments. However, by knowing the polymer molecular chemistry and structure and the exact nature of the oxidation reaction, it is possible to identify the molar volume of oxygen required for complete oxidation reaction of a given volume of a polymer. This would be a single parameter measuring the total volume of oxygen required for the complete oxidation of a unit polymer volume. In the absence of such chemical characterization, indirect relationships and bulk measurements are necessary and practical. However, as can be seen from the simulations presented here, simple linear and static (age independent) relationships between reaction rate and weight loss rate may not be adequate, as there may be multiple chemical mechanisms such as chain secession and hydrolysis occurring simultaneously with an impact on weight loss. Although we do not present a direct correlation with known physical or chemical mechanisms, the experimental results by Ripberger et al. [16] indicate that the weight loss rate decreases sharply with aging time during the initial aging period and approach a plateau value for longer aging times. It is therefore, reasonable to assume that the proportionality constant α is larger at the beginning of oxidation and decreases with aging time. For this work, we assume a linear relation for α for the first 40 h of aging which leads to numerical predictions of oxidation layer growth which correlate well with experimental measurements for 500 h of aging. Parametric studies indicate that a further reduction in α is needed for good comparisons at longer aging times.

While the experimentally observed layer growth with optical measurement of layer size compares reasonably with the simulations, complications arise in such correlation due to material loss, cracking and material shrinkage at longer durations of exposure. In this study the diffusivity of the oxidized material is inferred by comparing the model response to the oxidation layer thickness measurements obtained from isothermal (at 288 °C (550 °F)) aging experiments. Although the increased diffusivity with oxidation is physically intuitive, a direct measurement of the diffusivity is a superior observation. Such measurements are currently precluded by difficulties in processing thin films on which diffusivity measurements could be made. Efforts are currently underway to process thin films made of PMR-15 polyimide resins and measure the diffusivity values of completely oxidized films and compare them with the estimations reported in this work. Direct measurement of diffusivity of the oxidized and unoxidized polymers and composites is also complicated by the thermo-oxidation reaction which accompanies the diffusion.

Acknowledgements

The authors gratefully acknowledge the support from the Air Force Office of Scientific Research under the MEANS-I program (with Dr. Charles Lee as the Program Manager). Particular thanks are due to Mr. Erik Ripberger, AFRL/MLSA and Mr. Josh Briggs of UDRI for their help with aging experiments.

References

[1] Abdeljaoued K. Thermal oxidation of PMR-15 polymer used as a matrix in composite materials reinforced with carbon fibers. Ph.D. thesis, Ecole Nationale Superieure des Arts et Metiers, Paris; 1999.
[2] Bowles KJ, Jayne D, Leonhardt TA. Isothermal aging effects on PMR-15 resin. SAMPE Quarterly 1993;24(2):2–9.
[3] Bowles KJ, Papadopoulos DS, Inghram LL, McCorkle LS, Klan OV. Longtime durability of PMR-15 matrix polymer at 204, 260, 288 and 316 °C. NASA/TM-2001-210602; 2001.
[4] Celina M, Wise J, Ottesen DK, Gillen KT, Clough RL. Correlation of chemical and mechanical property changes during oxidative degradation of neoprene. Polymer Degradation and Stability 2000;68:171–84.
[5] Colin X, Marais C, Favre JP. Damage/weight loss relationship of polymer matrix composites under thermal aging. In: Massard T, Vautrin A, editors. Proceedings of ICCM-12. ICCM Europe Publications; 1999. CDrom, paper # 311.
[6] Colin X, Marais C, Verdu J. Thermal oxidation kinetics for a poly(bismaleimide). Journal of Applied Polymer Science 2001;82(14):3418–30.
[7] Colin X, Marais C, Verdu J. A new method for predicting the thermal oxidation of thermoset matrices: application to an amine crosslinked epoxy. Polymer Testing 2001;20(7):795–803.
[8] Colin X, Marais C, Verdu J. Kinetic modeling and simulation of gravimetric curves: application to the oxidation of bismaleimide and epoxy resins. Polymer Degradation and Stability 2002;78:545–53.
[9] Colin X, Verdu J. Thermal aging and lifetime prediction for organic matrix composites. Plastics, Rubber and Composites 2003;32(8–9): 349–56.
[10] Colin X, Verdu J. Strategy for studying thermal oxidation of organic matrix composites. Composites Science and Technology 2005;65:411–9.
[11] Decelle J, Huet N, Bellenger V. Oxidation induced shrinkage for thermally aged epoxy networks. Polymer Degradation and Stability 2003;81: 239–48.
[12] Gillen KT, Wise J, Clough RL. General solution for the basic autoxidation scheme. Polymer Degradation and Stability 1995;47:149–61.
[13] Meador MAB, Lowell CE, Cavano PJ, Herrera-Fierro P. On the oxidative degradation of nadic endcapped polyimides: I. Effect of thermocycling on weight loss and crack formation. High Performance Polymers 1996;8: 363–79.
[14] McManus HL, Foch BJ, Cunningham RA. Mechanism-based modeling of long-term degradation. Journal of Composites Technology and Research 2001;22(3):146–52.
[15] Nam JD, Seferis JC. Anisotropic thermo-oxidative stability of carbon-fiber reinforced polymeric composites. SAMPE Quarterly 1992;24(1): 10–8.
[16] Ripberger E, Tandon GP, Schoeppner GA. Characterizing oxidative degradation of PMR-15 resin. Proceedings of the SAMPE 2004 symposium/ exhibition, Long Beach, CA; May 16–20, 2004 [ITAR restricted].
[17] Salin IM, Seferis JC. Anisotropic effects in thermogravimetry of polymeric composites. Journal of Polymer Science 1993;31:1019–27.
[18] Schoeppner GA, Curliss DB. Model-based design for composites life management. 9th AIAA/ISSMO symposium on multidisciplinary analysis and optimization. Paper # 5516; 2002.
[19] Schoeppner GA, Tandon GP. Aging and durability of PMR-15 high temperature polyimide. Proceedings 35th international SAMPE technical conference, Dayton, OH; Sept. 28–Oct. 2, 2003.
[20] Tsuji LC, McManus HL, Bowles KJ. Mechanical properties of degraded PMR-15 resin. NASA technical report 1998-208487; 1998. p. 1–18.
[21] Wang SS, Chen X, Skontorp A. High temperature mechanics modeling and experiments of thermal oxidation, degradation and damage evolution in carbon fiber/polyimide composites. Proceedings of American Society for Composites 18th technical conference, University of Florida, Gainesville, FL; Oct. 19–22, 2003.
[22] Wise J, Gillen KT, Clough RL. Quantitative model for the time-dependent of diffusion-limited oxygen profiles. Polymer 1997;38: 1929–44.